Evaluation of 6-^{11}C-Methyl-*m*-Tyrosine as a PET Probe for Presynaptic Dopaminergic Activity: A Comparison PET Study with β-^{11}C-L-DOPA and ^{18}F-FDOPA in Parkinson Disease Monkeys

Masakatsu Kanazawa[1], Hiroyuki Ohba[1], Norihiro Harada[1], Takeharu Kakiuchi[1], Shin-ichi Muramatsu[2], and Hideo Tsukada[1]

[1]*Central Research Laboratory, Hamamatsu Photonics K.K., Hamamatsu, Shizuoka, Japan; and* [2]*Division of Neurology, Department of Medicine, Jichi Medical University, Tochigi, Japan*

We recently developed a novel PET probe, 6-^{11}C-methyl-*m*-tyrosine (^{11}C-6Me*m*Tyr), for quantitative imaging of presynaptic dopamine synthesis in the living brain. In the present study, ^{11}C-6Me*m*Tyr was compared with β-^{11}C-L-DOPA and 6-^{18}F-fluoro-L-dopa (^{18}F-FDOPA) in the brains of normal and Parkinson disease (PD) model monkeys (*Macaca fascicularis*). **Methods:** PD model monkeys were prepared by 1-methyl-4-phenyl-1,2,3,6-tetrahydropyridine (MPTP) administration, and ^{11}C-β-CFT was applied to assess neuronal damage as dopamine transporter (DAT) availability. ^{11}C-6Me*m*Tyr, β-^{11}C-L-DOPA, or ^{18}F-FDOPA was injected with and without carbidopa, a specific inhibitor of peripheral aromatic L-amino acid decarboxylase. In normal and PD monkeys, the dopamine synthesis rates calculated using PET probes were analyzed by the correlation plot with DAT availability in the striatum. **Results:** In normal monkeys, whole-brain uptake of β-^{11}C-L-DOPA and ^{18}F-FDOPA were significantly increased by carbidopa at the clinical dose of 5 mg/kg by mouth. In contrast, ^{11}C-6Me*m*Tyr was not affected by carbidopa at this dose, and the metabolic constant value of ^{11}C-6Me*m*Tyr in the striatum was significantly higher than those of the other 2 PET probes. Significant reduction of the presynaptic DAT availability in the striatum was detected in MPTP monkeys, and correlation analyses demonstrated that ^{11}C-6Me*m*Tyr could detect dopaminergic damage in the striatum with much more sensitivity than the other PET probes. **Conclusion:** ^{11}C-6Me*m*Tyr is a potential PET probe for quantitative imaging of presynaptic dopamine activity in the living brain with PET.

Key Words: dopamine; Parkinson's disease; 6-^{11}C-methyl-*m*-tyrosine; β-^{11}C-L-DOPA; ^{18}F-FDOPA

J Nucl Med 2016; 57:303–308
DOI: 10.2967/jnumed.115.161802

Parkinson disease (PD) provides progressive degradation of nigrostriatal pathways with selective loss of the dopaminergic neurons in the substantia nigra pars compacta (SNc), resulting in movement disorders such as resting tremor, akinesia, bradykinesia, rigidity, and postural instability. These clinical symptoms of PD were induced after 40%–50% loss of the dopaminergic neurons in the SNc and the reduction of dopamine in the striatum to about 20% of normal levels (*1*). Although the direct cause of this selective neurodegeneration in PD is not clearly understood, mitochondrial dysfunction has emerged as a common aspect of the pathogenesis (*2,3*).

Brain abnormality of PD patients has been imaged with PET as impaired presynaptic dopamine parameters such as dopamine synthesis, dopamine transporter (DAT), and vesicular monoamine transporter availabilities, as well as tentatively upregulated postsynaptic dopamine D_2 receptor binding at the initial stage (*4*). Dopamine synthesis capacity is regulated by DOPA concentration. PD syndromes are ameliorated by L-DOPA administration, suggesting that lowered dopamine neuronal activity can be overcome by a higher level of L-DOPA, Our previous study using L-β-^{11}C-DOPA (*5*) demonstrated that 6R-L-erythro-5,6,7,8-tetrahydrobiopterin, a cofactor for tyrosine hydroxylase (TH), could increase the striatal dopamine synthesis in normal monkey brain (*6*). 6-^{18}F-fluoro-L-dopa (^{18}F-FDOPA) has widely been applied for clinical diagnosis of the presynaptic dopamine function using PET. It has been assumed that ^{18}F-FDOPA follows the same transport, synthetic, and metabolic pathways of dopamine (*7*). ^{18}F-FDOPA uptake reflects the activity of aromatic L-amino acid decarboxylase (AADC) in the nerve terminals of the nigrostriatal dopaminergic pathway, and the metabolized ^{18}F-fruoro-dopamine (^{18}F-FDA) is stored in the vesicles through vesicular monoamine transporter. We have applied β-^{11}C-L-DOPA (*5*) to monitor dopamine synthesis rate facilitated by pharmacologic manipulations in normal monkeys (*6,8,9*) as well as impaired (*10*) in 1-methyl-4-phenyl-1,2,3,6-tetrahydropyridine (MPTP)–treated PD model monkeys (*11*). Because these research studies required multiparametric PET assessments of presynaptic dopamine synthesis, DAT, and postsynaptic dopamine receptors in the same subject in a day, the short half-life of ^{11}C is very useful for the repeated PET measurements. In contrast, the labeling by multienzymatic reactions limits the availability of β-^{11}C-L-DOPA only in the limited PET facilities (*5*).

Despite the usefulness of ^{18}F-FDOPA PET for the diagnosis of PD patients (*4,12*), ^{18}F-FDOPA is not always an ideal PET probe. One reason is that because ^{18}F-FDA is taken into the vesicles in presynaptic dopaminergic terminals, released, and metabolized further, its signal is influenced by both vesicular uptake and release processes (*13*). Another reason is caused by the peripheral decarboxylation by

Received Jun. 2, 2015; revision accepted Oct. 22, 2015.
For correspondence contact: Hideo Tsukada, Central Research Laboratory, Hamamatsu Photonics K.K., 5000 Hirakuchi, Hamakita, Shizuoka 434-8601, Japan.
E-mail: tsukada@crl.hpk.co.jp
Published online Nov. 12, 2015.

AADC and the methylation at the 3-hydroxyl group by catechol *O*-methyl transferase (COMT). The resulting ^{18}F-3-*O*-Me-FDOPA crosses the blood–brain barrier by the large neutral amino acid transporter (*14*), thereby worsening the signal-to-noise ratio and complicating kinetic modeling (*15,16*). A further limitation is due to the radiolabeling production of ^{18}F-FDOPA with electrophilic reactions using molecular ^{18}F-F_2 or ^{18}F-acetylhypofuorite (*17*) and nucleophilic reactions with no-carrier-added ^{18}F-fluoride (*18,19*). The former reactions provide the low radioactivity yields with low specific radioactivity, and the latter ones are concerned with the complex multistep reactions and enantiomeric purity.

6-^{18}F-fluoro-L-*m*-tyrosine (^{18}F-F*m*T) has been proposed for presynaptic dopamine imaging (*20–23*). ^{18}F-F*m*T is decarboxylated to 6-^{18}F-fluoro-*m*-tyramine (^{18}F-F*m*TA) by AADC with a 10-fold-greater affinity than ^{18}F-FDOPA (*21*). ^{18}F-F*m*TA has a 3-fold-greater affinity for monoamine oxidase-A than ^{18}F-FDA, and 6-^{18}F-fluoro-3-hydroxyphenylacetic acid (^{18}F-FHPAA) is trapped in the striatum (*21*). ^{18}F-F*m*TA and ^{18}F-FHPAA were also produced by peripheral AADC and monoamine oxidase-A, respectively, in plasma; however, these metabolites of ^{18}F-F*m*T cannot cross the blood–brain barrier (*24*). Methylated metabolites of ^{18}F-F*m*T are not formed because ^{18}F-F*m*T does not have the catechol structure for a substrate of COMT. These metabolic properties can make the signal of ^{18}F-F*m*T fully representing the extent of AADC activity with better quality than L-DOPA–based PET probes. However, the long half-life of ^{18}F prevents repeated PET measurements of pre- and postdrug treatments in the same subject in a day.

We developed a ^{11}C-labeled PET probe, 6-^{11}C-methyl-*m*-tyrosine (^{11}C-6Me*m*Tyr), for quantification of presynaptic dopamine activity (*25*). In the present study, ^{11}C-6Me*m*Tyr was compared with β-^{11}C-L-DOPA and ^{18}F-FDOPA in the monkey brain (*Macaca fascicularis*). The effects of carbidopa, a peripheral AADC inhibitor, on the brain uptake of these PET probes were assessed in normal animals. Furthermore, in PD animals, dopaminergic neuronal damage induced by MPTP was determined as DAT availability measured using ^{11}C-β-CFT (*26*), and sensitivity of each PET probe to dopaminergic neuronal damage was evaluated by correlation plot analyses with DAT availability.

MATERIALS AND METHODS

Animals and Drugs

Animals were maintained and handled in accordance with the recommendations of the U.S. National Institutes of Health and the guidelines of the Central Research Laboratory, Hamamatsu Photonics. This experiment was approved by the Ethical Committee of the Central Research Laboratory, Hamamatsu Photonics.

MR images of the monkeys were obtained with a 3.0-T MR imager (Signa Excite HDxt 3.0T; GE Healthcare) using a 3-dimensional spoiled gradient echo sequence (176 slices with a 256 × 256 image matrix; slice thickness/spacing, 1.4/0.7 mm; echo time, 3.4–3.6 ms; repetition time, 7.7–8.0 ms; inversion time, 400 ms; and flip angle, 15°) under pentobarbital anesthesia.

Isoflurane and pancronium were purchased from Sumitomo Dainippon Pharma Co. Ltd. and Daiichi Sankyo Co. Ltd., respectively. Kryptofix222 (K[2,2,2]), *N*-(diphenylmethylene)glycine *tert*-butyl ester, and MPTP were from Sigma-Aldrich Japan. The enzymes for β-^{11}C-L-DOPA synthesis, alanine racemase (EC 5.1.1.1.), D-amino acid oxidase (EC1.4.3.3.), and β-tyrosinase (EC 4.1.99.2.) were purchased from lkeda Food Research. 6-nitoroveratraldehyde and (*R,R*)-3,4,5-trifluorophenyl-NAS bromide were obtained from Tokyo Chemical Industry Co. Ltd. and Wako Pure Chemical Industries Ltd., respectively. Fluoro-dopamine (FDA) was from ABX GmbH. Precursors of ^{11}C-6Me*m*Tyr, ^{18}F-FDOPA, and ^{11}C-β-CFT; their corresponding standard compounds; and 6-Me-*m*-tyramine (6Me*m*TA), 6-Me-*m*-hydroxyphenylacetic acid (6MHPAA), and 3-*O*-Me-FDOPA were purchased from NARD Institute Ltd.

PET Ligand Syntheses

Positron-emitting ^{11}C and ^{18}F were produced by ^{14}N(p,α)^{11}C and ^{18}O(p, n)^{18}F nuclear reactions, respectively, using the cyclotron (HM-18; Sumitomo Heavy Industry, Ltd.) at the Hamamatsu Photonics PET center.

^{11}C-6Me*m*Tyr was labeled using a rapid Pd(0)-mediated cross-coupling reaction of ^{11}C-methyl iodide and corresponding alkenyl boronate precursor (*25*). The synthesis time was 35 min from an end of bombardment. The radiochemical purity was better than 99%, and the specific radioactivity was 40.0 ± 10.1 GBq/μmol.

β-^{11}C-L-DOPA was synthesized using a combination of organic synthesis and multienzymatic procedures (*5*). The radiochemical purity was better than 98%, and the specific radioactivity was 25.4 ± 8.5 GBq/μmol.

^{18}F-FDOPA was labeled by a highly enantioselective synthesis method using chiral phase-transfer alkylation (*19*). The radiochemical purity was greater than 99%, and the specific radioactivity was 47.0 ± 13.9 GBq/μmol.

^{11}C-β-CFT for DAT was labeled by ^{11}C-*N*-methylation of its nor-compound with ^{11}C-methyl iodide (*26*). The radiochemical purity was greater than 98%, and the specific radioactivity was 42.0 ± 7.9 GBq/μmol.

PD Monkey Model

Cynomolgus monkeys weighing 2.0–3.5 kg were used for PD model preparation (*10,11*). MPTP at doses ranging from 0.2 to 0.4 mg/kg of free base in phosphate-buffered saline was injected intravenously once per week over a 4-mo period until a stable parkinsonian syndrome was observed. The total dose of MPTP administered was 1.5 and 3.0 mg/kg.

PET Measurements

Four normal and 4 MPTP monkeys underwent PET scans using ^{11}C-6Me*m*Tyr, β-^{11}C-L-DOPA, and ^{18}F-FDOPA, all of which were obtained with and without carbidopa (5 mg/kg, by mouth, 1 h before probe injection), and ^{11}C-β-CFT under isoflurane anesthetic state. For more comparison of carbidopa effects, 4 normal monkeys were analyzed using ^{11}C-6Me*m*Tyr and ^{18}F-FDOPA after carbidopa administrations at 0.15 and 5 mg/kg, intravenously, 1 h before probe injection. After overnight fasting, monkeys were tracheostomized, immobilized with 0.05 mg/kg intramuscularly of pancronium bromide every 2 h, and artificially ventilated (Cato; Dräger). Anesthesia was continued with 0.8 volume % isoflurane in a $N_2O/O_2/N_2$ (1:1:1) gas mixture during the entire experiment. A venous cannula for PET ligand injection was inserted. The mean arterial blood pressure, heart rate, rectal temperature, arterial PO_2 and PCO_2, and pH were continuously or regularly monitored. The animal's body temperature was maintained within normal limits with a heating blanket. The animal was placed supine with a head holder in the PET gantry with stereotactic coordinates aligned parallel to the OM plane. After a transmission scan for 30 min, emission scans were obtained for 91 min using an animal PET scanner (SHR-7700; Hamamatsu Photonics) (*27*). The PET data were reconstructed by the filtered backprojection method with a Hanning filter of 4.5 mm in full width at half maximum and attenuation correction using the transmission scan data.

Volumes of interest (VOIs) in brain regions were drawn manually on the MR image according to regional information from BrainMaps.org (*28*), and VOIs of MR images were superimposed on the coregistered PET images to measure the time–activity curves of each PET probe for kinetic analyses.

PET Data Analysis

The quantitative analyses of ^{11}C-6Me*m*Tyr, β-^{11}C-L-DOPA, and ^{18}F-FDOPA were performed by a multitime graphical analysis (MTGA)

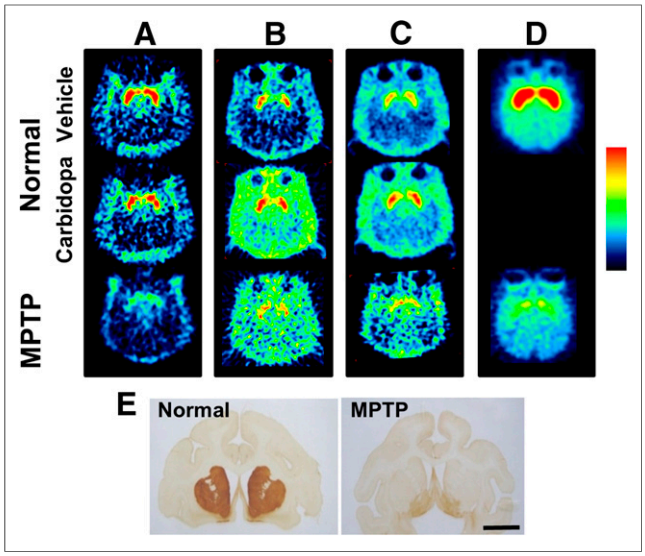

FIGURE 1. Typical PET images of ^{11}C-6Me*m*Tyr (A), β-^{11}C-L-DOPA (B), ^{18}F-FDOPA (C), and ^{11}C-β-CFT (D) in brains of normal and MPTP-treated monkeys. For PET imaging from A to D, vehicle or carbidopa at clinical dose of 5 mg/kg by mouth was administered. PET scans were conducted for 91 min with each PET probe, and SUV images from 62 to 91 min after injection were reconstructed from A to E. Immunohistologic analyses were performed using anti-TH antibody and brain slices of normal and MPTP-treated monkeys (E).

(*29–31*) using PMOD software (PMOD Technologies Ltd.) applying the time–activity curve in the cerebellum as an input function.

The analysis of ^{11}C-β-CFT was conducted by nondisplaceable binding potential (BP_{ND}) analysis (*32*) using PMOD software. As an input function, the time–activity curve in the cerebellum was applied.

Metabolic Analyses

A radio–thin-layer chromatography method was used to evaluate the effects of carbidopa on the metabolic profiles of ^{11}C-6Me*m*Tyr and ^{18}F-FDOPA in plasma. Arterial blood samples were obtained from monkeys at 5, 15, 30, 60, and 90 min after the injection of each PET probe and centrifuged at 12,000 rpm for 3 min to separate plasma. Ethanol was added to the plasma (plasma/ethanol = 1:2 (v/v)) followed by centrifugation. The obtained supernatants were developed with $CHCl_3$/n-BuOH/CH_3COOH/H_2O (2:3:1:1) for ^{11}C-6Me*m*Tyr or n-BuOH/CH_3COOH/H_2O (4:1:1) for ^{18}F-FDOPA, respectively, and exposed to a phosphoimaging plate. The plate was measured with FLA-7000 (Fujifilm Corp.).

Immunohistochemical Assessment

Monkeys were perfused with 4% paraformaldehyde through the ascending aorta under anesthesia with an overdose sodium pentobarbital. The brains were removed and cut into blocks 5 mm thick. These blocks were postfixed, left for 3 d in phosphate-buffered saline containing 30% sucrose, and cut into coronal sections 30 μm thick. Sections were treated with 0.3% H_2O_2 for 15 min to inhibit endogenous peroxidase. Sections were incubated at 48°C for 2 d in phosphate-buffered saline containing 0.3% Triton X-100 and primary antibodies against mouse monoclonal anti-TH antibody (1:8,000). Sections were incubated with biotinylated antimouse IgG (1:1,000) for 1 h at room temperature and in avidin–biotin–peroxidase complex (1:50) for 30 min at room temperature. Peroxidase activity was revealed in 50 mM Tris-HCl buffer (pH 7.6) containing 0.0004% H_2O_2 and 0.01% diaminobenzidine.

Statistical Analysis

Results are expressed as mean ± SD. Comparisons between conditions were performed using the paired, 2-tailed Student *t* test. A probability level of less than 5% ($P < 0.05$) was considered to indicate statistical significance.

RESULTS

As shown in the uppermost panels of Figures 1A–1C, each SUV image of ^{11}C-6Me*m*Tyr (Fig. 1A), β-^{11}C-L-DOPA (Fig. 1B), and ^{18}F-FDOPA (Fig. 1C) clearly showed the presynaptic dopamine synthesis activity in the striatum of normal monkey brain, and PET images of ^{11}C-6Me*m*Tyr provided high SUV in the striatum with best contrast between thestriatum and cortical regions, even without carbidopa administration. After the preadministration of carbidopa at 5 mg/kg by mouth shown in the middle panels of Figures 1A–1C, the uptake of β-^{11}C-L-DOPA (Fig. 1B) and ^{18}F-FDOPA (Fig. 1C) was increased not only in the striatal and cortical regions but also outside the skull. In contrast, no uptake changes in ^{11}C-6Me*m*Tyr were observed in the cortical regions by carbidopa (Fig. 1A).

Figure 2 shows time–activity curves of ^{11}C-6Me*m*Tyr (Fig. 2A), β-^{11}C-L-DOPA (Fig. 2B), and ^{18}F-FDOPA (Fig. 2C) in the striatal and cerebellar regions of normal monkey brain with and without carbidopa. Without carbidopa, time–activity curves of ^{11}C-6Me*m*Tyr reached a peak within 10 min in the striatum and within 5 min in the cerebellum after the injection, followed by the gradual clearance from the striatum and rapid from the cerebellum (Fig. 2A). Time–activity curves of β-^{11}C-L-DOPA (Fig. 2B) and ^{18}F-FDOPA (Fig. 2C) showed much lower peak values with much slower kinetics in the monkey brain than those of ^{11}C-6Me*m*Tyr

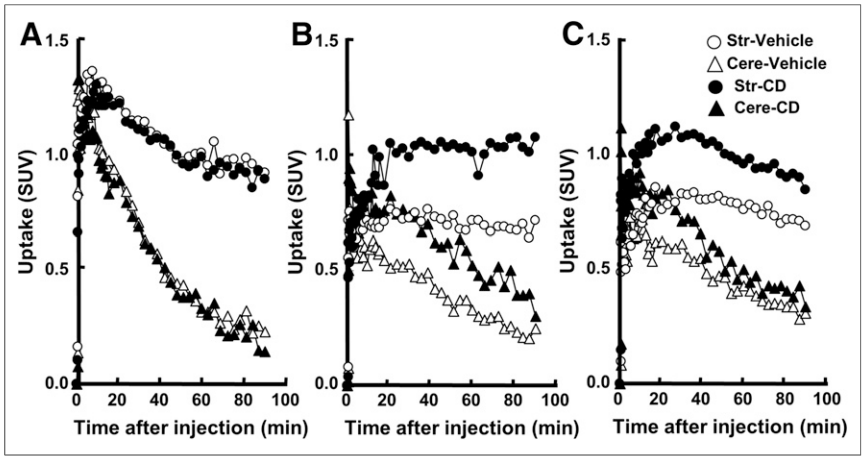

FIGURE 2. Effects of carbidopa (CD) at 5 mg/kg by mouth on time–activity curves of ^{11}C-6Me*m*Tyr (A), β-^{11}C-L-DOPA (B), and ^{18}F-FDOPA (C) in normal monkey brains. PET scans were conducted for 91 min with each PET probe. SUV images from 62 to 91 min after injection were reconstructed from A to C, and VOIs of striatum and cerebellum were set on PET images aided by MRI to obtain time–activity curves of each PET probe. Uptake values in each VOI were converted to SUVs.

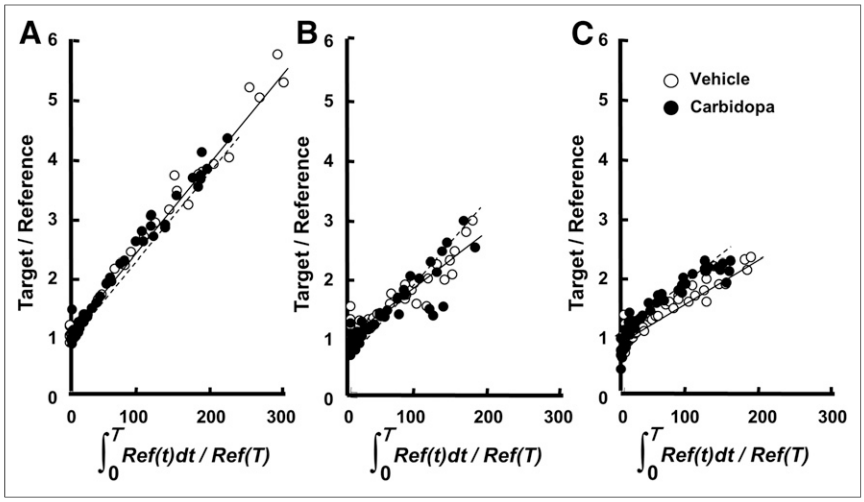

FIGURE 3. MTGA of ^{11}C-6Me*m*Tyr (A), β-^{11}C-L-DOPA (B), and ^{18}F-FDOPA (C) in normal monkey brains. PET scans were conducted for 91 min with each PET probe, and time–activity curves of SUVs in striatum and cerebellum were obtained as done in Figure 3.

(Fig. 2A). The preadministration of carbidopa at 5 mg/kg by mouth resulted in the higher peak values as well as slower kinetics of β-^{11}C-L-DOPA (Fig. 2B) and ^{18}F-FDOPA (Fig. 2C) than those in control. In contrast, the kinetics of ^{11}C-6Me*m*Tyr in the striatum and cerebellum were not affected by carbidopa (Fig. 2A).

As shown in Figure 3, MTGA demonstrated that ^{11}C-6Me*m*Tyr (Fig. 3A), β-^{11}C-L-DOPA (Fig. 3B), and ^{18}F-FDOPA (Fig. 3C) provided linear regression curves in the striatum. The slopes were highest for ^{11}C-6Me*m*Tyr, middle for β-^{11}C-L-DOPA, and lowest for ^{18}F-FDOPA without carbidopa, and those of β-^{11}C-L-DOPA and ^{18}F-FDOPA were shifted by carbidopa.

As shown in Figure 4, metabolic analyses of ^{11}C-6Me*m*Tyr and ^{18}F-FDOPA in plasma without carbidopa indicated that the proportion of unmetabolized ^{18}F-FDOPA to total radioactivity (Fig. 4D) was markedly lower than that of ^{11}C-6Me*m*Tyr (Fig. 4A) 15 min and thereafter. The preadministration of carbidopa increased this proportion of unmetabolized ^{18}F-FDOPA (Fig. 4D) and also increased that of metabolized ^{18}F-3-*O*-Me-FDOPA (Fig. 4E) by not only intravenous but also mouth administrations. The metabolic profile of ^{11}C-6Me*m*Tyr was affected by the intravenous administration of carbidopa, whereas the alteration degrees with by-mouth administration in the ratios of unmetabolized ^{11}C-6Me*m*Tyr (Fig. 4A), metabolized ^{11}C-6Me*m*TA (Fig. 4B), and ^{11}C-6MHPAA (Fig. 4C) were much lower than those of ^{18}F-FDOPA.

In terms of MTGA metabolic constant (Ki) values of the striatum calculated using a time–activity curve in the cerebellum as an input function, ^{11}C-6Me*m*Tyr was the highest, β-^{11}C-L-DOPA was middle, and ^{18}F-FDOPA was the lowest in normal animals (Fig. 5A). The SUV images (Fig. 1) and MTGA Ki values (Fig. 5A) revealed significant reduction of a presynaptic parameter of dopamine synthesis in the striatum of MPTP monkeys using ^{11}C-6Me*m*Tyr (Ki = 0.015 min^{-1} for normal and 0.007 min^{-1} for MPTP), β-^{11}C-L-DOPA (0.010 and 0.007 min^{-1}, respectively), and ^{18}F-FDOPA (0.007 and 0.006 min^{-1}, respectively). The most marked reduction by MPTP-induced dopamine damage was detected by ^{11}C-6Me*m*Tyr, namely, 46.6% of that of normal animals (Fig. 5A). The levels of Ki values of MPTP-treated monkeys were 58.2%, 66.7%, and 83.1% of their corresponding normal animals, for β-^{11}C-L-DOPA, and for ^{18}F-FDOPA, respectively (Fig. 5A).

When a presynaptic parameter of DAT availability was assessed using BP_{ND} of ^{11}C-β-CFT, it remarkably decreased in the striatum of MPTP monkeys (44.7% of that of normal animals) (Fig. 5B), which was supported by immunohistologic assessment using anti-TH antibody (Fig. 1E). Although plotting of the striatal MTGA Ki values of ^{11}C-6Me*m*Tyr, β-^{11}C-L-DOPA, or ^{18}F-FDOPA against BP_{ND} of ^{11}C-β-CFT in the striatum of normal and MPTP monkeys

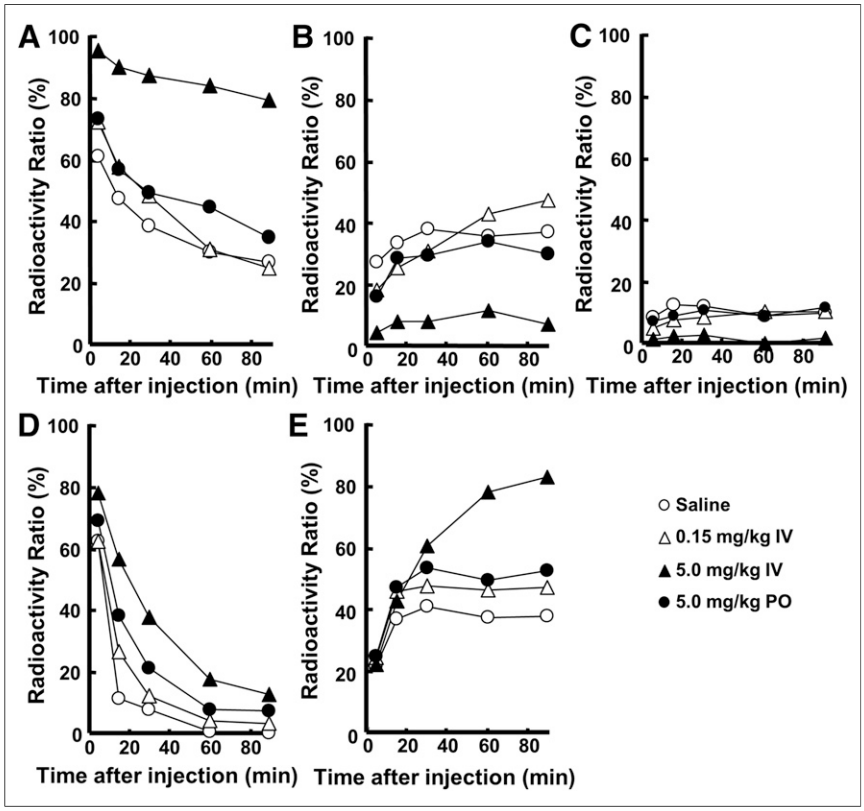

FIGURE 4. Effects of intravenous administration of carbidopa on metabolic profiles of ^{11}C-6Me*m*Tyr (A–C) and ^{18}F-FDOPA (D and E), in normal monkey plasma. Arterial blood samples were obtained from monkeys, and obtained plasma supernatants were applied on radio–thin-layer chromatography to analyze metabolic profiles of ^{11}C-6Me*m*Tyr (A), ^{11}C-6Me*m*TA (B), ^{11}C-6MHPAA (C), ^{18}F-FDOPA (D), and ^{18}F-3-*O*-Me-FDOPA (E). IV = intravenously; PO = by mouth.

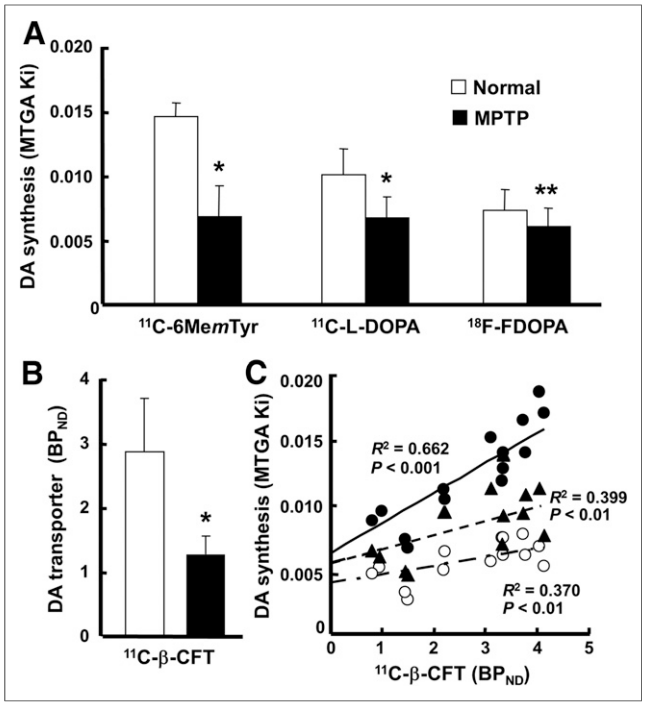

FIGURE 5. Effects of MPTP treatment on MTGA Ki values of ^{11}C-6Me*m*Tyr, β-^{11}C-L-DOPA, and ^{18}F-FDOPA (A); BP_{ND} values of ^{11}C-β-CFT (B); and correlations of MTGA Ki values of ^{11}C-6Me*m*Tyr, β-^{11}C-L-DOPA, or ^{18}F-FDOPA against BP_{ND} of ^{11}C-β-CFT (C) in monkey brains. BP_{ND} and MTGA Ki values were calculated using each time–activity curve in cerebellum as input function. ● = ^{11}C-6Me*m*Tyr; ▲ = β-^{11}C-L-DOPA; ○ = ^{18}F-FDOPA. $^{*}P < 0.01$ vs. each normal condition. $^{**}P < 0.05$ vs. each normal condition.

demonstrated significant positive correlations, Ki values of ^{11}C-6Me*m*Tyr provided greater correlation coefficients with BP_{ND} of ^{11}C-β-CFT than any other PET probes evaluated in the present study (Fig. 5C).

DISCUSSION

When β-^{11}C-L-DOPA or ^{18}F-FDOPA was injected into monkeys, the preadministration of carbidopa, at a clinical dose of 5 mg/kg by mouth, increased the uptake of radioactivity into the whole brain. As typically demonstrated using ^{18}F-FDOPA, this increased brain uptake was induced by the increase in brain-available radiolabeled compounds (the parent compounds themselves and corresponding 3-*O*-methyl-metabolites) by shifting to COMT metabolism in plasma by the AADC inhibition. In contrast, although the chemical structure of ^{11}C-6Me*m*Tyr raised the expectation that it is a substrate of peripheral AADC for decarboxylation to facilitate the brain uptake by carbidopa, it was not significantly affected by a clinical by-mouth dose of carbidopa. Previous studies using ^{18}F-F*m*T demonstrated that the administration of carbidopa increased the level of ^{18}F-F*m*T in plasma only by 15% (*24*) and also that the products of AADC-mediated decarboxylation were detected in plasma even with carbidopa administration (*33*). To assess the substrate specificity of ^{11}C-6Me*m*Tyr to AADC, carbidopa was intravenously administered to achieve higher plasma concentration than clinical by-mouth administration. As a result, the plasma level of ^{11}C-6Me*m*Tyr was increased and its metabolites, ^{11}C-6Me*m*TA and ^{11}C-6MHPAA, were decreased in a dose-dependent manner, suggesting that ^{11}C-6Me*m*Tyr could also be a substrate of peripheral AADC. The plasma metabolic analyses of ^{11}C-6Me*m*Tyr revealed that the inhibitory action of AADC by carbidopa at 5 mg/kg by mouth may be comparable to that determined by its intravenous administration at 0.15 mg/kg, both of which could be too low to affect the brain uptake of ^{11}C-6Me*m*Tyr in the living brain. Taken together, ^{11}C-6Me*m*Tyr should be useful as a PET probe for presynaptic dopamine imaging, because it can provide the sufficiently high Ki values in the striatum of the living brain even without carbidopa, and its MTGA Ki value was as high as that of ^{18}F-F*m*T in the monkey brain (*22*).

Because 3-*O*-methyl metabolites of L-DOPA in plasma are known to cross the blood–brain barrier into the brain, the COMT products of L-DOPA–based PET probes, β-^{11}C-L-DOPA and ^{18}F-FDOPA, resulted in the higher background activity in nondopamine regions than that of ^{11}C-6Me*m*Tyr. Among these 3 probes, ^{18}F-FDOPA revealed the lowest detection capability for MPTP-induced dopaminergic neuronal impairment in the living monkey brain. The metabolisms were substantially different between β-^{11}C-L-DOPA and ^{18}F-FDOPA in plasma; thus, ^{18}F-FDOPA is less stable with more production of its 3-*O*-methyl metabolite than ^{3}H/^{11}C-L-DOPA in the plasma of rats (*7,34*) and monkeys (*6,35*). Metabolic analyses of rat brain homogenates indicated that the radioactivity of L-^{11}C-*O*-methyl-DOPA contributed 17% of total radioactivity at 40 min after the injection of β-^{11}C-L-DOPA (*36*), whereas ^{18}F-*O*-methyl-FDOPA from ^{18}F-FDOPA contributed about 40%–50% (*37*), resulting in the low MTGA Ki value of ^{18}F-FDOPA. In contrast, because, along with no *O*-methyl-metabolite by COMT, the peripherally produced metabolites of ^{11}C-6Me*m*Tyr, ^{11}C-6Me*m*TA, and ^{11}C-6MHPAA may not cross the blood–brain barrier assumed from the metabolism of structure-relevant ^{18}F-F*m*T in plasma (*24*), the time–activity curve data exhibited the rapid and efficient clearance of its unconverted ^{11}C-6Me*m*Tyr from nondopamine regions in the brain resulting in the high MTGA Ki value of ^{11}C-6Me*m*Tyr. ^{18}F-F*m*T is decarboxylated to ^{18}F-F*m*TA by AADC in brain tissue, which has low affinity for the vesicular transporter, and is oxidized and trapped in axon terminals as ^{18}F-FHPAA by monoamine oxidase-A without being released or processed further (*20*). The metabolic analysis of ^{11}C-6Me*m*Tyr in the brain has not been conducted yet, but its metabolic analysis in plasma may be assumed to follow the same metabolic fate as ^{18}F-F*m*T.

Because AADC is present in the terminals of all monoaminergic neurons, the uptake of ^{18}F-DOPA, ^{11}C-6Me*m*Tyr, and β-^{11}C-L-DOPA into extrastriatal regions provides an index of the density of not only the dopamine, but also the serotonergic and noradrenergic terminals (*38*). However, when applied to assess density in the striatal regions, these uptake indices could exclusively be defined as the AADC activity of dopaminergic neurons. This interpretation is strongly supported by the present results that the striatal dopamine synthetic indices measured using these 3 probes were markedly decreased after the treatment by MPTP, a dopaminergic neuron-specific toxin; and MPTP-induced reduction degrees of striatal dopamine syntheses were significantly correlated with those of DAT availability. The present study applied ^{11}C-β-CFT, a DAT PET probe, as the gold standard for presynaptic dopamine function, for correlation analyses with each PET probe for dopamine synthesis. MTGA Ki values of ^{11}C-6Me*m*Tyr revealed a greater correlation coefficient to the degrees of dopaminergic neuronal activity than any of the other 2 PET probes. One reason for this result could be a common metabolic property among β-^{11}C-L-DOPA and ^{18}F-FDOPA, with catechol structure for a substrate of COMT. In contrast, because the ^{11}C-6Me*m*Tyr does not have a catechol structure for the 3-*O*-methyl reaction, the present result should be reasonable from a kinetic point

of view. The improved uptake constant of ^{11}C-6Me*m*Tyr is also expected to result in its improved sensitivity to changes in presynaptic dopaminergic function compared with β-^{11}C-L-DOPA and ^{18}F-FDOPA.

CONCLUSION

The present study demonstrated that ^{11}C-6Me*m*Tyr could be a potential PET probe for quantitative imaging of the presynaptic dopamine activity in the living brain with PET. Noninvasive assessment of AADC activity using ^{11}C-6Me*m*Tyr could be useful for diagnosis, prognosis, and treatment monitoring of diseases related to impaired presynaptic dopamine function.

DISCLOSURE

The costs of publication of this article were defrayed in part by the payment of page charges. Therefore, and solely to indicate this fact, this article is hereby marked "advertisement" in accordance with 18 USC section 1734. No potential conflict of interest relevant to this article was reported.

ACKNOWLEDGMENTS

We gratefully acknowledge the technical assistance of Shingo Nishiyama, Dai Fukumoto, Aiko Iwazaki, and Naomi Takino.

REFERENCES

1. Lees AJ, Hardy J, Revesz T. Parkinson's disease. *Lancet.* 2009;373:2055–2066.
2. Schapira AHV, Cooper JM, Dexter D, Clark JB, Jenner P, Marsden CD. Mitochondrial complex I deficiency in Parkinson's disease. *J Neurochem.* 1990;54: 823–827.
3. Swerdlow RH, Parks JK, Miller SW, et al. Origin and functional consequences of the complex I defect in Parkinson's disease. *Ann Neurol.* 1996;40:663–671.
4. Brooks DJ. Imaging approaches to Parkinson disease. *J Nucl Med.* 2010;51:596–609.
5. Bjurling P, Watanabe Y, Oka S, Nagasawa T, Yamada H, Långström B. Multienzymatic synthesis of β-^{11}C-labelled L-tyrosine and L-DOPA. *Acta Chem Scand.* 1990;44:183–188.
6. Tsukada H, Lindner KJ, Hartvig P, et al. Effect of 6R-L-erythro-5,6,7,8-tetrahydrobiopterin and infusion of L-tyrosine on the in vivo L-[β-^{11}C]DOPA disposition in the monkey brain. *Brain Res.* 1996;713:92–98.
7. Melega WP, Luxen A, Perlmutter MM, Nissenson CHK, Phelps ME, Barrio JR. Comparative *in vivo* metabolism of 6-[^{18}F]fluoro-Ldopa and [^{3}H]L-dopa in rats. *Biochem Pharmacol.* 1990;39:1853–1860.
8. Tsukada H, Harada N, Nishiyama S, Ohba H, Kakiuchi T. Cholinergic neuronal modulation alters dopamine D_2 receptor availability in vivo by regulating receptor affinity induced by facilitated synaptic dopamine turnover: PET studies with microdialysis in the conscious monkey brain. *J Neurosci.* 2000;20:7067–7073.
9. Tsukada H, Harada N, Nishiyama S, et al. Ketamine decreased striatal [^{11}C] raclopride binding with no alteration in static dopamine concentrations in the striatal extracellular fluid in the monkey brain: multi-parametric PET studies combined with microdialysis analysis. *Synapse.* 2000;37:95–103.
10. Muramatsu S, Okuno T, Suzuki Y, et al. Multitracer assessment of dopamine function after transplantation of embryonic stem cell-derived neural stem cells in a primate model of Parkinson's disease. *Synapse.* 2009;63:541–548.
11. Burns RS, Chiueh CC, Markey SP, Ebert MH, Jacobowitz DM, Kopin IJ. A primate model of parkinsonism: selective destruction of dopaminergic neurons in the pars compacts of the substantia nigra by MPTP. *Proc Natl Acad Sci U S A.* 1983;80:4546–4550.
12. Kuwabara H, Cumming P, Yasuhara Y, et al. Regional striatal DOPA transport and decarboxylase activity in Parkinson's disease. *J Nucl Med.* 1995;36:1226–1231.
13. Sossi V, de La Fuente-Ferna'ndez R, Holden JE, et al. Increase in dopamine turnover occurs early in Parkinson's disease: evidence from a new modeling approach to PET ^{18}F-fluorodopa data. *J Cereb Blood Flow Metab.* 2002;22: 232–239.
14. Kumakura Y, Vernaleken I, Gründer G, Bartenstein P, Gjedde A, Cumming P. PET studies of net blood-brain clearance of FDOPA to human brain: age-dependent decline of [^{18}F]fluorodopamine storage capacity. *J Cereb Blood Flow Metab.* 2005;25:807–819.
15. Reith J, Dyve S, Kuwabara H, Guttman M, Diksic M, Gjedde A. Blood-brain transfer and metabolism of 6-[^{18}F]fluoro-Ldopa in rat. *J Cereb Blood Flow Metab.* 1990;10:707–719.
16. Doudet DJ, McLellan CA, Carson R, et al. Distribution and kinetics of 3-*O*-methyl-6-[^{18}F]fluoro-l-DOPA in the rhesus monkey brain. *J Cereb Blood Flow Metab.* 1991;11:726–734.
17. Luxen A, Guillaume M, Melega WP, Pike VW, Solin O, Wagner R. Production of 6-[^{18}F]fluoro-L-dopa and its metabolism in vivo: a critical review. *Int J Rad Appl Instrum B.* 1992;19:149–158.
18. Lemaire C, Damhaut P, Plenevaux A, Comar D. Enantioselective synthesis of 6-[fluorine-18]-fluoro-L-dopa from no-carrier-added fluorine-18-fluoride. *J Nucl Med.* 1994;35:1996–2002.
19. Lemaire C, Gillet S, Guillouet S, Plenevaux A, Aerts J, Luxen A. Highly enantioselective synthesis of no-carrier-added 6-[^{18}F]fluoro-L-dopa by chiral phase-transfer alkylation. *Eur J Org Chem.* 2004;2004:2899–2904.
20. Jordan S, Eberling JL, Bankiewicz KS, et al. 6-[^{18}F]fluoro-L-*m*-tyrosine: metabolism, PET kinetics, and MPTP lesions in primates. *Brain Res.* 1997;750:264–276.
21. DeJesus OT. Positron-labeled DOPA analogs to image dopamine terminals. *Drug Dev Res.* 2003;59:249–260.
22. Eberling JL, Bankiewicz KS, O'Neil JP, Jagust WJ. PET 6-[^{18}F]fluoro-L-*m*-tyrosine studies of dopaminergic function in human and nonhuman primates. *Front Hum Neurosci.* 2007;1:9.
23. Boulton AA, Juorio AV. Cerebral decarboxylation of *meta* and para-tyrosine. *Experientia.* 1983;39:130–134.
24. Wahl LM, Chen JJ, Thompson M, Chirakal R, Nahmias C. The time course of metabolites in human plasma after 6-[^{18}F]fluoro-L-*m*-tyrosine administration. *Eur J Nucl Med.* 1999;26:1407–1412.
25. Kanazawa M, Ohba H, Iwazaki A, Kakiuchi T, Tsukada H. Synthesis of 6-^{11}C-methyl-*m*-tyrosine (^{11}C-6Me*m*Tyr) for dopamine synthesis imaging in living brain using PET. *Bioorg Med Chem.* 2015;23:729–734.
26. Dannals RF, Neumeyer JL, Milius RA, Ravert HT, Wilson AA, Wagner HN. Synthesis of a radiotracer for studying dopamine uptake sites in vivo using PET: 2β-carbomethoxy-3β- (4-fluorophenyl)-[N-^{11}C-methyl]tropane) ([^{11}C]CFT or [^{11}C]WIN 35,428). *J Labelled Comp Radiopharm.* 2006;33:147–152.
27. Watanabe M, Okada H, Shimizu K, et al. A high resolution animal PET scanner using compact PS-PMT detectors. *IEEE Trans Nucl Sci.* 1997;44: 1277–1282.
28. Jones EG, Stone JM, Karten HJ. High-resolution digital brain atlases: a Hubble telescope for the brain. *Ann N Y Acad Sci.* 2011;1225(suppl1):E147–E159.
29. Gjedde A. Calculation of cerebral glucose phosphorylation from brain uptake of glucose analogs in vivo: a re-examination. *Brain Res.* 1982;257:237–274.
30. Patlak CS, Blasberg RG. Graphical evaluation of blood-to-brain transfer constants from multiple-time uptake data: generalizations. *J Cereb Blood Flow Metab.* 1985;5:584–590.
31. Gjedde A, Reith J, Dyve S, et al. Dopa decarboxylase activity of the living human brain. *Proc Natl Acad Sci USA.* 1991;88:2721–2725.
32. Innis RB, Cunningham VJ, Delforge J, et al. Consensus nomenclature for in vivo imaging of reversibly binding radioligands. *J Cereb Blood Flow Metab.* 2007;27: 1533–1539.
33. Barrio JR, Huang S-H, Yu D-C, et al. Radiofluorinated L-*m*-tyrosines: new in-vivo probes for central dopamine biochemistry. *J Cereb Blood Flow Metab.* 1996;16:667–678.
34. Tsukada H, Lindner KJ, Hartvig P, et al. Effect of 6R-L-erythro-5,6,7,8-tetrahydrobiopterin on in vivo L-[β-^{11}C]DOPA turnover in the rat striatum with infusion of L-tyrosine. *J Neural Transm Gen Sect.* 1994;95:1–15.
35. Torstenson R, Tedroff J, Hartvig P, Fasth K-J, Långström B. A comparison of ^{11}C-labeled L-DOPA and L-fluorodopa as positron emission tomography tracers for the presynaptic dopaminergic system. *J Cereb Blood Flow Metab.* 1999;19: 1142–1149.
36. Lindner KJ, Hartvig P, Tedroff J, Ljungstrom A, Bjurling P, Långström B. Liquid chromatographic analysis of brain homogenates and microdialysates for the quantification of L-[β-^{11}C]DOPA and its metabolites for the validation of positron emission tomography studies. *J Pharm Biomed Anal.* 1995;13: 361–367.
37. Cumming P, Boyes BE, Martin WRW, et al. The metabolism of [^{18}F]6-fluoro-L-3,4-dihydroxy- phenylalanine in the hooded rat. *J Neurochem.* 1987;48:601–608.
38. Pavese N, Brooks DJ. Imaging neurodegeneration in Parkinson's disease, *Biochim Biophys Acta.* 2009;1792:722–729.